© 2007 International Society for Analytical Cytology

Original Articles

Fully Automated Segmentation and Morphometrical Analysis of Muscle Fiber Images

Yoo-Jin Kim,[1]* Thomas Brox,[2] Wolfgang Feiden,[1] and Joachim Weickert[3]

[1]Institute of Neuropathology, Saarland University, School of Medicine, Homburg/Saar, Germany
[2]Computer Vision and Pattern Recognition Group, University of Bonn, Germany
[3]Mathematical Image Analysis Group, Saarland University, Saarbrücken, Germany

Received 18 November 2005; Revision Received 23 June 2006; Accepted 7 July 2006

Background: Measurement of muscle fiber size and determination of size distribution is important in the assessment of neuromuscular disease. Fiber size estimation by simple inspection is inaccurate and subjective. Manual segmentation and measurement are time-consuming and tedious. We therefore propose an automated image analysis method for objective, reproducible, and time-saving measurement of muscle fibers in routinely hematoxylin-eosin stained cryostat sections.

Methods: The proposed segmentation technique makes use of recent advances in level set based segmentation, where classical edge based active contours are extended by region based cues, such as color and texture. Segmentation and measurement are performed fully automatically. Multiple morphometric parameters, i.e., cross sectional area, lesser diameter, and perimeter are assessed in a single pass. The performance of the computed method was compared to results obtained by manual measurement by experts.

Results: The correct classification rate of the computed method was high (98%). Segmentation and measurement results obtained manually or automatically did not reveal any significant differences.

Conclusions: The presented region based active contour approach has been proven to accurately segment and measure muscle fibers. Complete automation minimizes user interaction, thus, batch processing, as well as objective and reproducible muscle fiber morphometry are provided. © 2007 International Society for Analytical Cytology

Key terms: automated morphometry; image analysis; segmentation; muscle fiber size

In the assessment of muscular pathology, muscle fiber size and size distribution exhibit basic morphologic as well as diagnostic information. Abnormal deviations, such as atrophy or hypertrophy, are difficult to assess subjectively and it is useful to measure morphometrical parameters in hundreds of fibers, in order to compare these with normal data (1,2). It is also important to analyze histological sections quantitatively, since it has been shown that morphometric data can discern very early changes in the distribution pattern of fiber size in muscle biopsy samples (3). The estimation of muscle fiber size by simple inspection—as yet performed in routine diagnostics—is difficult and inaccurate. Practical techniques have included direct measurement using an eye piece micrometer measurement of a projected image or enlarged microphotographs. However, the manual morphometric approach and interpretation of muscle biopsy material is a subjective, tedious, and time-consuming task (4,5). In addition, reliable assessment of morphometric data in muscle biopsy samples is complicated by the necessity of measurements in several different fields within the biopsy in order to avoid selection bias. In view of these impracticable requirements, muscle fiber morphometry may be accomplished most reasonably by automated routines. Automated analysis of muscle fiber images has not yet received much attention and only few segmentation techniques are at hand so far. The reported methods are based on border

Parts of the method described in this paper were presented at the Annual Meeting of the Reference Centre for Neuromuscular Diseases of the German Society of Neuropathology and Neuroanatomy (DGNN) in April 2005, Aachen, Germany as well as at the Bildverarbeitung für die Medizin (BVM) 2006 Workshop, March 2006, Hamburg, Germany.

*Correspondence to: Yoo-Jin Kim, Institute of Neuropathology, Saarland University, School of Medicine, Bldg. 90.3, D-66421 Homburg/Saar, Germany.
E-mail: yoo.jin.kim@uniklinik-saarland.de

Published online 9 January 2007 in Wiley InterScience (www.interscience.wiley.com).
DOI: 10.1002/cyto.a.20334

WILEY InterScience® DISCOVER SOMETHING GREAT

shape enhancement routines, followed by application of user-defined or histogram-based thresholds, and interactive manual editing. The usability and performance of these semi-automated methods are still limited by inaccurate delineation of fibers as well as the need of special histochemical stains and user interaction (4,6,7). In contrast to these pixel intensity- and pixel gradient-based applications, Klemenčič et al. (8) suggested a semi-automated approach based on active contour models. The practicability of this method is restricted by the need of pointing the approximate centroid of each fiber manually by the investigator. We here propose a method that makes use of recent advances in level set based segmentation, where classical edge based active contours are extended by region based cues, such as the color and texture of the interior and exterior of the fiber regions. Whereas edge based active contours require an accurate contour initialization, which is usually provided by manual interaction, as in Ref. 8, region based active contours depend less on the initialization and can therefore ensure a reliable separation process without manual interaction. This leads to an accurate, fully automated methodology that allows for time-saving batch processing of the entire biopsy samples.

MATERIALS AND METHODS

Muscle Sample Preparation

Biopsy samples were trimmed, mounted, and frozen in isopentane-cooled liquid nitrogen, before storage at −70°C. Transverse sections (10 μm) were cut with a cryotome at −20°C and attached to slides by thawing. After keeping the slides at room temperature at least for 30 min., the sections were stained with hematoxylin and eosin.

Image Acquisition

Microscopic images were taken in artefact-free areas in muscle cross sections with a 20× objective (Nikon Eclipse E600 microscope, Nikon DN100 CCD-camera: Nikon, Tokio, Japan) and stored as 640 × 480 pixel (571 × 428 μm) RGB color images.

Segmentation Method

Combined region and edge based active contour model. The core algorithm for separating the muscle fibers from the connective tissue is based on active contour models as introduced by Kass et al. (9). The method makes use of the level set technique known from Refs. 10 and 11. Related level set based active contours are, in particular, edge based geodesic active contours (12,13) and region based active contours, as introduced by Chan and Vese (14) and Paragios and Deriche (15).

In level set based segmentation methods, the sought contour, which separates in this case the two classes of muscle fibers and connective tissue, is represented by the zero-level line of a so-called embedding function ϕ. This implicit representation of the contour has several advantages, among others that parts of the two regions need not necessarily be connected and that they can split and merge. This is essential for the present application, since the region of the muscle fibers itself consists of numerous so-called connected components separated from each other by areas of connective tissue, that is, it is not connected. For the analysis of the individual fibers it is even required that different fibers result in separated connected components.

Active contour models are variational models, that is, they are described by a cost functional $E(\phi)$, in which undesirable properties of a possible solution ϕ are penalized by high costs. By minimizing the total cost $E(\phi)$, one finds an optimal solution ϕ. In the active contour model used for our method, the energy consists of two parts:

$$E(\phi) = \underbrace{\int_{\Omega} (H(\phi)\log p_1 + (1 - H(\phi))\log p_2)dx}_{\text{Part I}} + \nu \underbrace{\int_{\Omega} g(\nabla I)|\nabla H(\phi)|dx}_{\text{Part II}}. \quad (1)$$

The first part is region based. Minimizing this part leads to a solution where all pixels within one region are maximally similar with respect to a certain similarity measure. This similarity measure is defined by the region models of the fibers and the tissue given by the probability density functions p_1 and p_2, respectively. The probability density functions are determined from the input image as described further below. The Heaviside function $H(\phi) = 1$ if $\phi > 0$ and $H(\phi) = 0$ if $\phi < 0$ is used to distinguish the two regions given the embedding function ϕ; see Ref. 14 for details.

The maximum similarity within regions has the natural consequence that there is additionally a maximum dissimilarity *between* the two regions. This part of the model exploits the fact that the muscle fibers all have a similar color that can generally be distinguished from the color of the intermyofibrillar connective tissue.

However, since the color alone may not always be sufficient to distinguish the two regions, especially because blood vessels can have a very similar color as the muscle fibers, the color information is supported by texture information derived by the method described in Ref. 16. The muscle fibers are mainly homogeneous without much textural variation, whereas the endomysial connective tissue contains collagenous fibers, blood vessels, fibrocytes, and other cellular components, which are captured by the texture features. Hence, taking also this texture information into account, leads to a more reliable separation of muscle fibers and intermyofibrillar tissue. The texture features used here basically model the magnitude, orientation, and scale of texture elements (16), which makes them similar to Gabor filter responses (17,18). In contrast to Gabor features, however, they

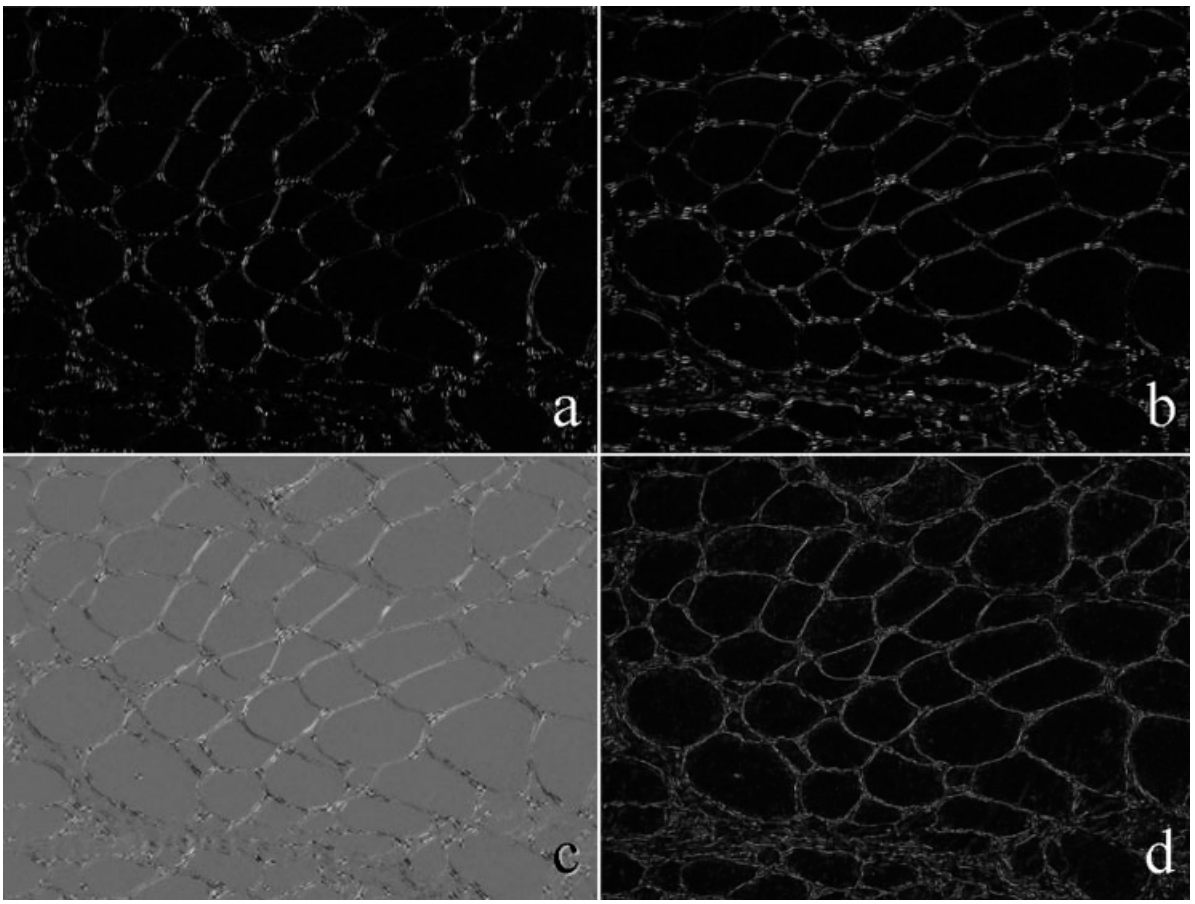

FIG. 1. Texture channels from Ref. 16 used in the active contour model. (**a**,**b**,**c**) Components of the structure tensor estimating magnitude and orientation of the texture. (**d**) Local scale measure estimating the scale of texture elements.

have a significantly lower redundancy and encode the texture information in only four channels. The extracted texture features for the sample image in Figure 2a are shown in Figure 1.

The three color channels and the additional four texture channels are combined in the joint probability density functions p_1 and p_2 involved in Eq. (1). The channels are assumed to be independent. Therefore, the probability densities for the fiber and non-fiber regions $i = 1$ and $i = 2$, respectively, can be computed as

$$p_i = \prod_{j=1}^{7} p_{ij} \tag{2}$$

The single channel probability densities p_{ij} are approximated with a Parzen density estimator (19–21), which comes down to computing a smoothed histogram in each region i and channel j.

The second part of the energy functional is edge based. Its influence relative to the first part is determined by the weighting parameter ν, which is empirically set to the fixed value $\nu = 2$. From the colored input image $I = (I_1,I_2,I_3)$ one can compute the inverse gradient magnitude:

$$g(\nabla I) = \frac{1}{\sqrt{\sum_{1}^{3}(\nabla I_k)^2 + 1}} \tag{3}$$

It serves as a weighting function that yields values close to 1 in homogeneous areas of the image and smaller positive values in the presence of edges. The contour that minimizes the second term in Eq. (1) is the curve of minimal weighted length. In other words, due to this term, the contour is attracted by edges and prefers to be as short as possible; for details see Refs. 12 or 13. This part of the model exploits the fact that the muscle fibers are often separated from the connective tissue by more or less strong edges. Hence it supplements a third cue for the partitioning besides the color and texture information. Moreover, the penalty on the contour length avoids single noise pixels or small artefacts to be separated from the surrounding region.

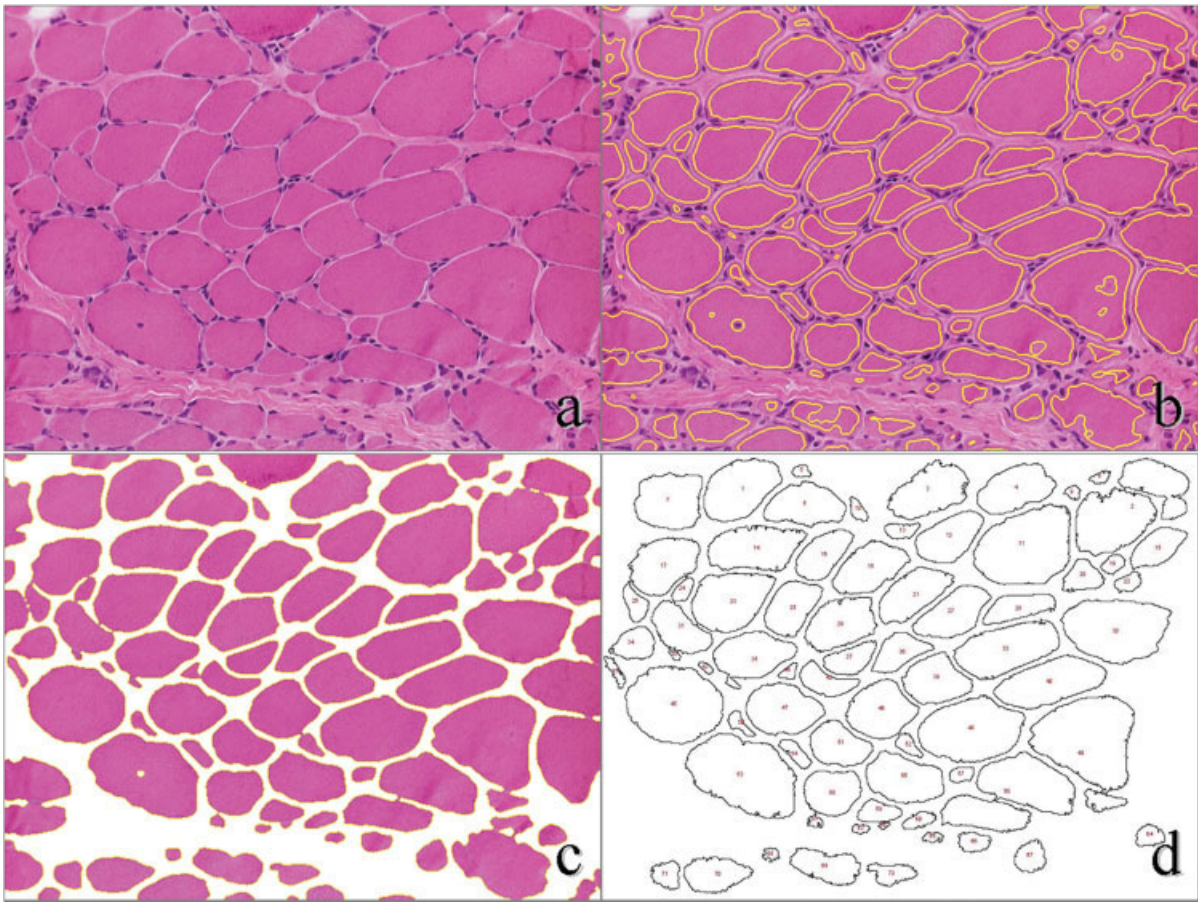

FIG. 2. (**a**) Original input RGB image of a dystrophic muscle biopsy sample (cryostat section, HE, ×20 objective). (**b**) Initial contour depicted in yellow. (**c**) Output image of the region based active contour model. The fiber contours are outlined and non-fiber structures are removed. Only myofibers are considered for further morphological processing. (**d**) Output image of analysis. Each analyzed fiber is outlined and numbered; fibers touching the image boundaries are not considered by the analysis routine. [Color figure can be viewed in the online issue, which is available at www.interscience.wiley.com]

In order to find the optimum solution according to the energy in Eq. (1), one starts with some initial partitioning and then performs a gradient descent that evolves the contour towards solutions with smaller energy. This is achieved by iteratively updating the embedding function, which comprises the contour as its zero-level line. The update in each iteration is determined by the gradient descent equation derived from the energy functional:

$$\phi^{k+1} = \phi^k + \tau \cdot H'(\phi^k) \cdot \left(\log \frac{p_1(\phi^k)}{p_2(\phi^k)} + \nu \cdot \mathrm{div}\left(g(\nabla I) \frac{\nabla \phi^k}{|\nabla \phi^k|} \right) \right) \quad (4)$$

where k denotes the iteration index and τ the iteration step size. $H\prime(\phi)$ is the derivative of a smoothed version of the Heaviside function (14). After 200 iterations with $\tau = 0.5$, one obtains the sought contour separating the muscle fibers from the connective tissue (see Fig. 1c). Computation times are below 2 min on contemporary hardware including texture feature computation.

Setting the initial contour. Due to the region based cues, the active contour model is significantly less sensitive to the initialization than purely edge based models. Nevertheless, one can slightly improve the segmentation result by setting the initialization with care. Furthermore, an initialization that is closer to the sought solution reduces the number of iterations necessary for convergence, and thus speeds up the algorithm. For these reasons, the initialization method makes use of two known facts: firstly, the myofibers capture more than half of the total area of the image and are rather homogeneously colored; secondly, the color of the myofibers is approximately determined by the preparation with hematoxylin and eosin. Therefore, all pixels with a color that is either closer to the histogram mode than a fixed threshold or closer to the a-priori known preparation color than a fixed threshold are initially assigned to the region of myofibers. All remaining pixels are assigned to the region of connective tissue. After this assignment, the embedding function is smoothed by a Gaussian kernel with standard deviation 2.5 in order to remove small enclosures in both regions. After this procedure, the initial contour, shown in Figure 2b, is in general already a good approximation of the final contour and less than 200 iterations are sufficient for the active contour to converge.

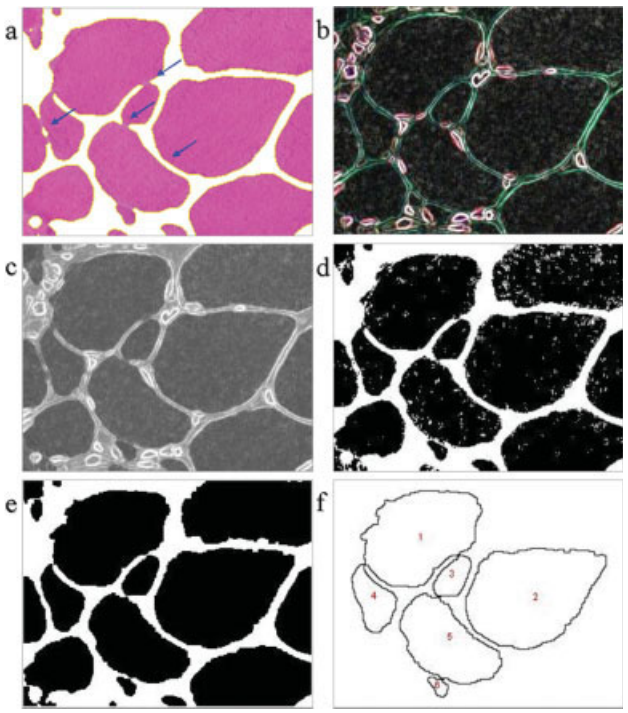

FIG. 3. Steps of refinement for separating adjacent fibers. (**a**) Detail from the active contour segmented image of a dystrophic muscle biopsy sample. Fiber boundaries are incompletely bordered in small areas where thin interfibrillar septa are still bridging adjacent fibers (arrows). (**b**) Edge-detected image serves as morphological mask with enhanced fiber boundaries. (**c**) Active contour segmented image (a) and edge-detector (b) are merged by extraction of average pixel values of both images resulting in a 8-bit image. (**d**) Binary image after application of mixture modeling and (**e**) morphological operations. Adherenced fibers are completely separated. (**f**) Output image after analysis. Each single fiber is correctly segmented and numbered. Edged fibers are excluded automatically from analysis. [Color figure can be viewed in the online issue, which is available at www.interscience.wiley.com]

Refining the segmentation result. Although the active contour model yields accurate boundaries in large parts of the image, some myofibers may not be completely separated from each other (Fig. 3a, arrows). Myofibers represent individual skeletal muscle cells. Therefore, the single fiber is well-defined to the surrounding connective tissue by a cell membrane, which causes the strong edges between the homogeneously textured myofibers and the fascicular arranged collagenous fibers of the connective tissue. Therefore, in order to refine the result, a Sobel operator is applied to the original image as edge detector (Fig. 3b) and serves as morphological filter which enhances the fiber outlines. The Sobel convolution kernel performs a 2D spatial gradient measurement on an image and so emphasizes regions of high spatial gradient that correspond to edges. The edge detector image is merged with the result of the active contour model in Figure 3a by extracting the average pixel values of all color channels in both images, resulting in a 8-bit grey value image (Fig. 3c). Each muscle fiber region is binarized by applying a threshold to the grey values of pixels forming the region (Fig. 3d). For thresholding, we used the mixture modeling method, which automatically selects the proper threshold. This method separates the histogram of an image into two classes using a Gaussian model and then calculates the image threshold as the intersection of these two Gaussians. The resulting binary image is then processed by operations of mathematical morphology (22): irregularities ("holes") within the segmented fibers are eliminated by outlining and refilling the outlined structures, whereas irregularities in the fiber contour are removed by applying the "opening" filter (erosion followed by dilation). The result of this morphological postprocessing is shown in Figure 3e.

The data flow diagram in Figure 4 gives an overview of the main steps of the proposed system.

Morphometric analysis. Different morphometrical parameters for each region of interest (segmented muscle fibers), that is, fiber cross-sectional area, perimeter, circularity, Feret diameter, and lesser diameter, are calculated automatically by built-in routines of ImageJ (Public Domain, http://rsb.info.nih.gov/ij/). Muscle fibers which are only partially engaged within the picture frame (edged particles) are excluded automatically from analysis. All analyzed fibers/structures are outlined, numbered, and displayed in the output image (Figs. 2d and 3f).

System Performance

A total of 30 digital images containing 679 fibers on five human muscle specimens were segmented by the automated method. The image data was derived from (1) two biopsy samples with no pathological alterations, one of those with very narrow distances between fibers or even partially touching fibers and with low grey value gradient between myofiber and interfibrillar connective tissue (Fig. 5a), (2) two samples with neurogenic atrophy, containing hypertrophic fibers and also nuclear clumps (Fig. 5c), (3) one dystrophic muscle sample with numerous strongly hypotrophic fibers and proliferation of connective tissue (Figs. 2, 3, and 5e), and segmentation results were evaluated independently by two neuropathologists (Y.-J.K. and W.F.), respectively. Each single object,

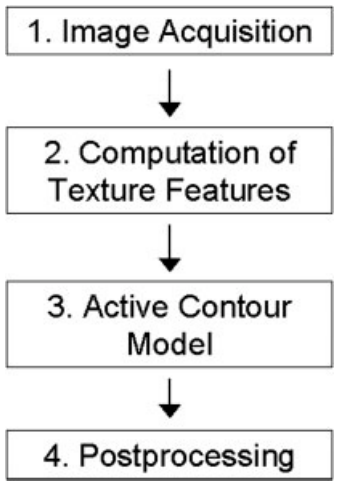

FIG. 4. Data flow diagram highlighting the main steps of the segmentation procedure.

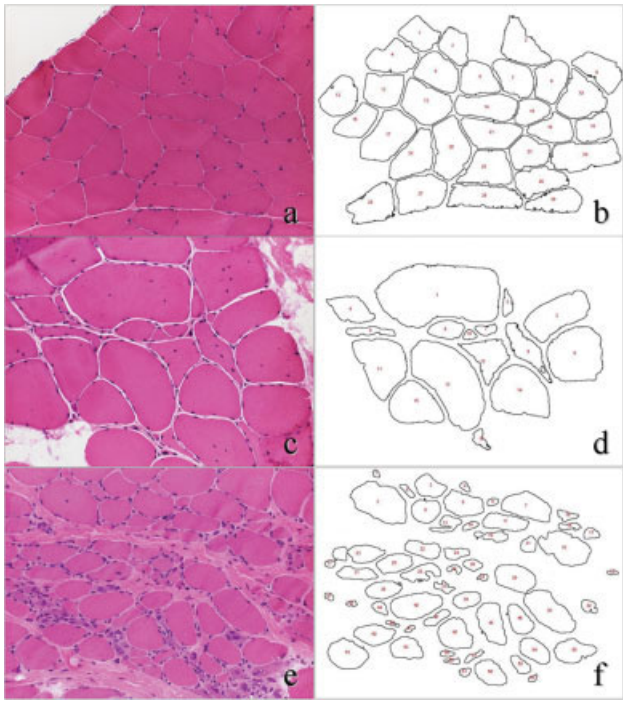

FIG. 5. Morphological variability among the tested image samples, HE, objective ×20. (**a**) Normal muscle biopsy sample. Intermyofibrillar septa are generally thin, some fibers are attached closely to each other. (**c**) Neurogenic alteration with grouped atrophy and compensatory hypertrophy. (**e**) Dystrophic muscle biopsy with high level of fiber atrophy and hypertrophy of connective tissue. (**b**,**d**,**f**) Corresponding output images of automated segmentation and analysis procedures. [Color figure can be viewed in the online issue, which is available at www.interscience.wiley.com]

which was regarded by the automated system as a single region of interest and which was concordantly assigned to a single myofiber by the experts were recorded as correctly detected - whereas each region of interest, which did not correspond to a single myofiber, that is, clustered myofibers, blood vessels, or connective tissue areas, was recorded as falsely segmented. The percentage of correctly detected fibers as displayed in the output images (Figs. 2d, 5b, 5d, and 5f) from the total amount of fibers (n = 679) was defined as correct classification rate. The inherent parameters of the methodology were kept fixed for all images to ensure a fully automated processing.

Additionally, the accuracy of the morphometric analysis was assessed by comparison between human and machine measurements of 10 out of the 30 digital images containing a total of 191 fibers on five human muscle specimens (normal, neurogenic atrophic, and dystrophic muscle samples as described above). Three experts traced fiber outlines with a computer mouse using the "freehand" ROI selection tool. Calculation of cross sectional area, perimeter, circularity, and Feret diameter were done automatically by the computer for each outlined fiber. The manually collected data were compared to the machine measurement of the same images and the segmented regions whether obtained by human or machine were compared directly with each other by calculating the percentage of overlapping pixels (overlap ratio). For each fiber, the three human measurements and the results obtained by the automated system were averaged. This was used as standard of comparison. The mean error was defined as the mean of deviations from the standard of comparison assessed for each fiber (Table 1).

RESULTS

The main steps of the segmentation process are illustrated in Figures 2 and 3. The example image taken from a dystrophic biopsy sample demonstrates the accurate distinction of myofibers from non-myogenic structures by the active contour model (Fig. 2c). In most cases, fiber boundaries are bordered accurately. However, particularly in moderately prepared specimens and highly dystrophic samples, some closely adherent fibers are not completely separated by the active contour. In the final refinement step of the segmentation procedure almost all of these small bridging areas between the fibers are eliminated by the application of the edge-detected image as morphological mask (Fig. 3b).

Direct comparison of the presented approach (Figs. 6b and 6d) with segmentation results obtained by alternative initialization (Figs. 6a and 6c) or active contour algorithm according to Chan and Vese (Fig. 6e) are displayed exemplarily in Figure 6. Obviously, the method is not very sensitive to different initializations. Although the initialization in Figure 6a leads to the false segmentation of some blood vessels at the boundary, most of the fibers are segmented correctly. On the other hand, the statistical model and the texture features involved are crucial to deal with such muscle fiber images, as the result obtained with the Chan–Vese method in Figure 6e reveals.

Additionally, a sensitivity analysis of the segmentation procedure was performed by adding noise to the original images (signal to noise ratio: 5.44). This still yielded accurate segmentation results (Fig. 6f), though the noise reduces the discriminative power of the texture features.

Table 1
Mean Overlap Ratios, Average Morphometrical Values, and Mean Error [%] From Standard of Comparison as Assessed for 191 Fibres, Obtained Manually by Three Investigators and by Machine

	Human 1	Human 2	Human 3	Machine
Overlap ratio	94.5%	95.4%	95.5%	94.3%
Fibre area	5,707 μm^2; 7.6%	5,639 μm^2; 7%	5,617 μm^2; 6.7%	5,625 μm^2; 7%
Perimeter	292.5 μm; 5.6%	301.1μm; 4.1%	301.1μm; 4.3%	302.7μm; 4%
Circularity	0.74; 6.1%	0.70; 9.7 %	0.69; 9.4 %	0.68; 10.5%
Diameter	111.3 μm; 3.7%	111.4 μm; 4.1%	110.9 μm; 3.5%	111 μm; 3.6%

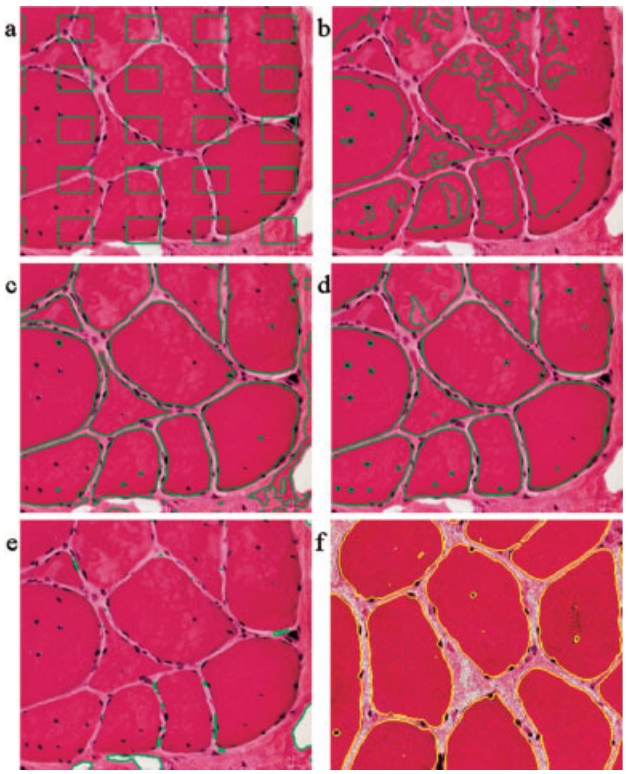

FIG. 6. Comparison of the proposed method with alternative initialization and segmentation result using the active contour model according to Chan and Vese, HE, objective ×20. (**a**) Alternative initialization, (**c**) proposed initialization, and (**b**,**d**) corresponding segmentation results. (**e**) Segmentaion result using the active contour model according to Chan and Vese applied to color images. (**f**) Segmentation result of the proposed model after adding noise to the original image (signal to noise ratio: 5.44). [Color figure can be viewed in the online issue, which is available at www.interscience.wiley.com]

Therefore, higher noise levels would decrease the ability of the method to separate single fibers.

The correct classification rate among a total of 679 fibers was high (663 fibers correctly detected: 98%). Neither the mean overlap ratios nor the morphometric data obtained manually or by the computerized automated method reveal any significant differences. Mean deviations of the morphometric parameters in each of the 191 fibers did not show any significant differences either (Table 1).

DISCUSSION

Despite a great demand for computerized automated procedures in muscle fiber morphometry, there are only few papers dedicated to this topic so far. To date, there are some segmentation approaches based on pixel-intensity and gradient information (4,6,7). In contrast to these semi-automatic segmentation methods, our results suggest that the combined edge and region based active contour approach is suitable for fully automated fiber segmentation and analysis. The accurate segmentation procedure and analysis performance of our automated method deplete the user interaction up to the level of visual supervision. The rate of correctly segmented fibers in our method is even better than in some semi-automatic methods and the performance of measurements is as accurate as manual analysis by experts. A previous prototype of an active contour based method as introduced by Klemenčič (8) also showed acceptable analysis performance, however, the practicability of this prototype was still limited by the necessity of extensive user interaction. First, in order to construct the Voronoi polygons, centroids had to be pointed manually for each fiber. This manual selection of centroids comprises subjectivity and presumes precognition as well as experiences in neuromuscular diagnostics. In our method, the initialization of the contour detection process is determined fully automatically by a histogram analysis and a thresholding procedure. This is possible, since region based active contours are less sensitive to bad initializations than their purely edge based predecessors and still yield reasonable results in cases where the initialization obtained with the thresholding is far from the sought solution. Consequently, a manual definition of fiber centroids is no longer necessary.

Second, Voronoi regions that are unbounded had to be outlined manually. Instead we proposed a refinement of the active contour result by an edge-enhanced mask, which finally leads to a high rate of correctly bounded fibers. Only few fibers in moderately prepared biopsy samples with no visible striplines to adjacent fibers or very thin intermyofibrillar septum with low gradients were falsely segmented and comprised merely 2% of all investigated fibers. Even in highly dystrophic muscle samples with great variations in fiber size and distribution, as well as hypertrophy of connective tissue, fatty degeneration, and amounts of terminally atrophic fibers, nuclear clumps, and regenerative alterations, the morphometric analyses were quite accurate and in direct comparison, the overlap ratios between manual and automatic segmentation results were high.

In muscle fiber image segmentation, the fundamental challenge to overcome is the separation of myofibers from non-fiber structures of same pixel-intensity or color. Intensity and gradient based methods do not consider further intrinsic myofiber-specific information, and therefore, structures like, that is, blood vessels, nuclear clumps, resorptive processes, and inflammatory infiltrates cannot be differed from muscle fibers. Since connective tissue may exhibit similar staining intensity and color, all conventional segmentation methods are restricted to staining for alkaline myosin adenosine-triphosphatase (ATPase) after preincubation at different pH, because the connective tissue is omitted by the ATPase reaction. However, other structures, in particular blood vessels, are also ATPase reactive, and therefore, segmentation results are still inaccurate. This leads to inappropriate segmentation and inaccurate measurement results, particularly in biopsy samples with pathological alterations. In order to cope with this challenge, the presented method exploits three sources of information to separate the classes: firstly, the myofibers can mostly be separated from the remaining tissue by means of the color, as provided by the sample preparation; secondly, the edge based term from classical active contours exploits the fact that muscle fibers are often

separated by more or less strong edges from the connective tissue; thirdly, the texture model respects that the fiber regions are almost homogeneous in contrast to the remaining tissue and thereby adds an additional source of information to the process that has not been taken into account by previous approaches. A further important feature of the proposed method is the implicit representation of the separating contour by a level set function that allows for topological changes. Consequently, the problem of separating a multitude of myofiber regions reduces to the much simpler task of separating the image into two classes, one that captures the area of the myofibers and one that captures the non-fiber structures. This classification approach enables a reliable and more practicable segmentation of myofibers - even in routinely HE-stained specimens.

In conclusion, the method will prove to be very valuable in high-content image analysis of muscle samples for research purposes as well as in clinical diagnostics. Since the method enables full automation, convenient batch processing of the entire biopsy sample may be possible, and therefore, selection bias could be avoided. The method is easy to use and it neither requests special knowledge in image processing nor special histochemical stains.

LITERATURE CITED

1. Swash M, Schwartz MS. Neuromuscular Diseases. Berlin: Springer; 1988.
2. Mastaglia FL. Skeletal Muscle Pathology. London: Churchill Livingstone; 1992.
3. Dubowitz V. Muscle Biopsy: A Practical Approach. London: Bailliere Tindall; 1985.
4. Castleman KR, Chui LA, Martin TP, Edgerton VR. Quantitative muscle biopsy analysis. Monogr Clin Cytol 1984;9:101–116.
5. Eilbert JL, Gallistel CR, McEachron DL. The variation in user drawn outlines on digital images: Effects on quantitative autoradiography. Comput Med Imaging Graph 1990;14:331–339.
6. Dudley AW, Spittal RM, Dayoff RE, Ledley RS.Computed image analysis techniques of skeletal muscle. In: Jasmin G, Proschek L, editors. Microanalysis and Quantification. Basel: Karger; 1984. pp 34–57.
7. Collumbien R, Zukowski F, Claeys A, Roels F. Automated analysis of muscle fibre images. Anal Cell Pathol 1990;2:373–387.
8. Klemenčič A, Kovačič S, Pernus F. Automated segmentation of muscle fiber images using active contour models. Cytometry 1998;32:317–326.
9. Kass M, Witkin A, Terzopoulos D. Snakes: Active contour models. Int J Comput Vision 1988;1:321–331.
10. Dervieux A, Thomasset F. A finite element method for the simulation of Rayleigh-Taylor instability. In: Rautman R, editor. Approximation Methods for Navier-Stokes Problems. Berlin: Springer; 1979. pp 145–158.
11. Osher S, Sethian JA. Fronts propagating with curvature-dependent speed: Algorithms based on Hamilton-Jacobi formulations. J Comput Phys 1988;79:12–49.
12. Caselles V, Kimmel R, Sapiro G. Geodesic active contours. Int J Comput Vision 1997;22:61–79.
13. Kichenassamy S, Kumar A, Olver P, Tannenbaum A, Yezzi A. Conformal curvature flows: From phase transitions to active vision. Arch Rational Mech Anal 1996;134:275–301.
14. Chan T, Vese L. Active contours without edges. IEEE Trans Image Proc 2001;10:266–277.
15. Paragios N, Deriche R. Geodesic active regions: A new paradigm to deal with frame partition problems in computer vision. J Vis Commun Image Represent 2002;13(1/2):249–268.
16. Brox T, Weickert J. A TV flow based local scale measure for texture discrimination. In: Pajdla T, Matas J, editors. Lecture Notes in Computer Science, Vol. 3022. Berlin: Springer; 2004. pp 578–590. Proceedings of the 8th European Conference on Computer Vision.
17. Gabor D. Theory of communication. J Inst Electr Eng 1946;93:429–457.
18. Bovik AC, Clark M, Geisler WS. Multichannel texture analysis using localized spatial filters. IEEE Trans Pattern Anal Mach Intell 1990; 12:55–73.
19. Parzen E. On the estimation of a probability density function and the mode. Ann Math Stat 1962;33:1065–1076.
20. Rousson M, Brox T, Deriche D. Active unsupervised texture segmentation on a diffusion based feature space. In: Proceedings of the IEEE Conference on Computer Vision and Pattern Recognition, Vol. 2, Madison, WI; 2003. pp 699–704.
21. Brox T, Rousson M, Deriche R, Weickert J. Unsupervised segmentation incorporating colour, texture, and motion. In: Petkov N, Westenberg MA, editors. Lecture Notes in Computer Science, Vol. 2756: Computer Analysis of Images and Patterns. Berlin: Springer; 2003. pp 353–360.
22. Soille P: Morphological Image Analysis. Berlin: Springer; 1999.